Draft version November 18, 2021
Typeset using LaTeX default style in AASTeX631

Stellar Peanuts: Binary Analysis of KIC 7766185

Conor M. Larsen[1]

[1] *Department of Astrophysics and Planetary Science*
Villanova University
800 E Lancaster Ave
Villanova, PA, 19085, USA

ABSTRACT

We present a detailed study of the contact binary KIC 7766185. Spectroscopic observations were conducted by the Mayall 4-m telescope at Kitt Peak National Observatory and used to create a radial velocity curve. Using the radial velocity curve and *Kepler* measurements, binary analysis in *PHOEBE* was conducted to determine system parameters and the first set of absolute stellar parameters. The absolute stellar parameters confirm KIC 7766185 as an A-type W UMa system. Along with the binary analysis, a period study was conducted. The O-C diagram determined that there are no current period variations. However, the study demonstrated that the ephemeris reported in the *Kepler Eclipsing Binary Catalog* is incorrect. We report a new value for the ephemeris of KIC 7766185.

Keywords: Eclipsing Binary Stars – Contact Binaries – Stellar Parameters – Individual: KIC 7766185

1. INTRODUCTION

Contact binaries include some of the most interesting and extreme binary star systems. In these systems, two stars orbit so close that they share a common envelope. Of the contact binaries, the most common type is the W UMa type stars, consisting of two late type stars (mostly of spectral type F, G and K) which have come in contact and share a common, convective envelope (Terrell et al. (2012)). The W UMa type stars are low mass and have relatively equal eclipse depths (Eker et al. (2008)).

The contact model for W UMa stars was first proposed by L.B. Lucy. His seminal paper, published in 1968, described the first complete theory of contact binaries (Lucy (1968)). Since this work, the de-facto explanation for contact binaries and W UMa stars is that the stars come in thermal and geometric contact. The origin and evolution of these objects is still unresolved. However, there is little doubt that angular momentum loss plays a role in formation. The current consensus states that contact binaries were initially detached binaries. Through angular momentum loss, and subsequent orbital decay, the stars migrate towards one another until contact is achieved (Ruciński (1986)). The exact mechanism of angular momentum loss is also an open question, however theorists have proposed mass loss via stellar wind, mass transfer and magnetic braking as potential explanations (Ruciński (1986); Gazeas & Stępień (2008)).

The stars in contact binaries are so close that tidal distortions become present. The gravitational and tidal interactions distort the two stars. Therefore, the two stars form a typical "peanut" shape. Figure 3 displays the model, created by this study, for the W UMa star KIC 7766185. The model clearly demonstrates the "stellar peanut" shape of W UMa stars.

Due to the contact between the stellar components, the stars in W UMa systems usually have the same temperature and luminosity, despite having different masses and radii. This property had been noted before the merging nature of contact binaries was realized (i.e., before Lucy's groundbreaking work) (Binnendijk (1965)). Once the stars come in geometrical contact, they come in thermal contact with one another. Once in thermal contact, thermal energy is transferred between the two stars, forcing the luminosity and temperature of the two objects to become relatively equivalent, within a few hundred kelvin (Csizmadia & Klagyivik (2004)). However, a sub-set of W UMa stars (B-type) has much greater temperature differences. B-type W UMa stars are in geometrical contact, but not thermal contact which allows the two stars to have vastly different temperatures. Generally, B-type systems are those which have a difference in surface temperature of more than 1000 K (Csizmadia & Klagyivik (2004)).

Parameter	Value	Reference
Distance	$933.881^{+25.168}_{-23.880}$ pc	1
Orbital Period	0.8354573 days	2
$T_{\rm eff}$	5977 K	2
log(g) in cgs units	4.280	2
E(B-V)	0.077	2
V-Filter Magnitude	12.02 ± 0.18	3
Spectral Type	F3V	4
T_2/T_1	0.97814	5
Mass Ratio	0.81789	5
Fillout Factor	0.18943	5
sin$i$	0.97737	5

Table 1. System Parameters of KIC 7766185. References: 1: *Gaia EDR3*, Brown et al. (2021). 2: *KIC*, Brown et al. (2011). 3: *Tycho-2 Catalog*, Høg et al. (2000). 4: Frasca, A. et al. (2016) 5: Prša et al. (2011)

W UMa stars have 3 sub-types based on temperature and size. A-type systems occur when the larger star is the hotter component, and W-type systems occur when the smaller star is the hotter component. As stated earlier, B-type systems occur when the temperature difference between the two stars is high, above 1000 K (Csizmadia & Klagyivik (2004)).

This study focuses specifically on the contact binary KIC 7766185. KIC 7766185 is a $12^{\rm th}$ magnitude system of spectral type F3V (Frasca, A. et al. (2016)). Certain parameters for this target were previously determined in large reviews of *Kepler* data (Prša et al. (2011); Frasca, A. et al. (2016)), however, there has yet to be an in-depth study focusing specifically on this target. A review of previously determined parameters of KIC 7766185 is presented in Table 1. Note that the values for effective temperature and log(g) are averages of the two stars obtained from spectroscopy at a random phase. Since the phase is unknown, the contribution of light by each individual star is unknown. Therefore, these values, obtained from the *Kepler Input Catalog* (*KIC*) (Brown et al. (2011)), are estimates of the average values of the two stars.

This paper will discuss the observations of KIC 7766185 (2.), the radial velocity measurements (3.), the binary analysis (4.), the period study (5.) and finally a discussion of the results (6.) and a conclusion (7.).

2. OBSERVATIONS

2.1. *Photometric Observations*

KIC 7766185 has been extensively observed by the *Kepler Space Telescope* (Borucki et al. (2010)). Several measurements were obtained between 2009 and 2013 which were utilized to create a phase folded light curve. The *Kepler* data was downloaded from the *Kepler Eclipsing Binary Catalog* (Prša et al. (2011)). The *Kepler* light curve is displayed in Figure 1. The light curve has rounded tops, a distinct feature of contact binaries. The primary and secondary eclipses are of relatively equal depth, indicating a temperature ratio close to 1. Since the eclipses are of equal depth and the system consists of late type stars, KIC 7766185 is a W UMa system. Clear outliers are visible in the light curve. Before analysis was conducted, the outliers were removed using the outlier removal function in the period analysis software *Peranso* (Paunzen & Vanmunster (2016)).

KIC 7766185 was also observed by the *Transiting Exoplanet Survey Satellite* (*TESS*) (Ricker et al. (2015)). Observations were conducted between July and August 2019 during *TESS* sector 14. During this sector, 28 days of measurements were completed. The binary analysis was conducted with the *Kepler* light curve only. The *TESS* measurements were only utilized for the period analysis section.

2.2. *Spectroscopic Observations*

Spectroscopic observations of KIC 7766185 were obtained by the Kitt Peak Mayall 4-m telescope located at Kitt Peak National Observatory, Arizona (KPNO (2021)). The measurements were obtained during an observing run dedicated to measuring spectra of W UMa type stars identified by *Kepler* (Proposal ID: 2010B-0434). The observations were conducted with a Tektronix 2048x2048 chip (T2KB) and the Echelle spectrograph (31.6 gratings/mm). The data files were obtained from the project PI (Dr. Andrej Prša, Villanova University). A total of 7 spectra were obtained between

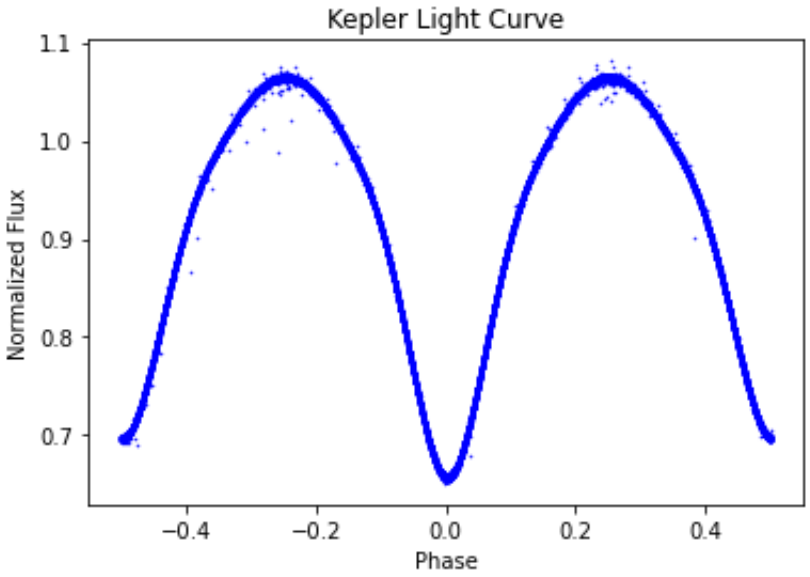

Figure 1. Light curve of KIC 7766185 created using *Kepler* data

September 26, 2010 and September 28, 2010. Each spectra was obtained with an exposure time of 600 seconds over a wavelength range of ∼4000 Å to ∼10000 Å. The 4 spectra obtained on September 26 and the one spectrum obtained on September 27 were maintained at a camera temperature of -77 °C. The 2 spectra obtained on September 28 were maintained at a camera temperature of -75 °C. The spectra were reduced through a pipeline before being obtained by the observing run PI. They were reduced in *IRAF* using the echelle package. The crreject algorithm was used to remove cosmic rays from the data (J. Orosz, personal communication, Nov. 8, 2021). One of the spectra is displayed in Figure 2. The deepest lines visible are due to telluric interference. The most prominent real absorption lines are the hydrogen Balmer lines at 6562 Å (H_α) and 4861 Å (H_β).

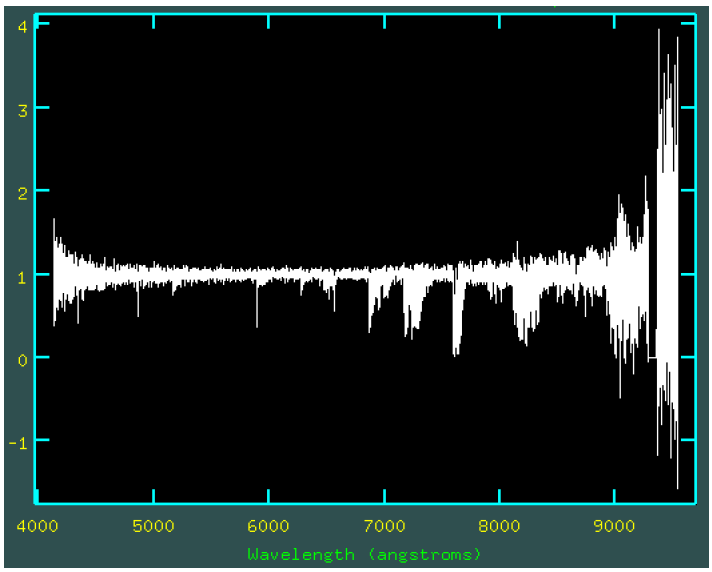

Figure 2. Example spectrum (Spectrum 4) obtained by the Mayall Telescope on September 26, 2010. The spectrum has been reduced and normalized.

Table 2 displays a list of the 7 spectra along with the corresponding Julian date and phase. The phase was calculated using the ephemeris and period listed in the *Kepler Eclipsing Binary Catalog*:

$$E = \frac{T_{obs} - T_0}{P} = \frac{T_{obs} - 2454954.554702}{0.8354573} \tag{1}$$

The integer part of E is the epoch and the decimal part of E is the phase.

Spectrum Number	Julian Date	Phase
1	2455465.63409722	0.736
2	2455465.73430057	0.856
3	2455465.79096064	0.924
4	2455465.8518264	0.997
5	2455466.81974781	0.155
6	2455467.80578357	0.336
7	2455467.83015266	0.365

Table 2. List of Spectra along with the Julian Date and phase of observation.

3. RADIAL VELOCITY MEASUREMENTS

Radial velocity measurements were obtained using the FXCOR task in *IRAF* (Tody (1986)). FXCOR is based off the Fourier cross-correlation method developed by Tonry & Davis (1979). An overview of FXCOR functionality and commands is given by Alpaslan (2009). FXCOR uses a template of known redshift to determine the shift in another spectrum. Fortunately, Spectrum 4 was obtained at a phase of 0.997, during the primary eclipse. During an eclipse there is no radial motion of the individual stars and therefore there is no shift in the atomic lines (except for the shift due to the movement of the entire system, discussed shortly). Spectrum 4 was utilized as the template to measure the shifts for the other spectra. By using one of the obtained spectra as a template, the systemic velocity cannot be determined, however, this information is not important for determining system parameters through binary analysis.

Each spectra was divided into 200 Å regions and run through FXCOR. The regions beyond 7000 Å were excluded as they are dominated by telluric interference. After running FXCOR on each range, the radial velocities were averaged and the standard deviation was calculated. For each range, the VHELIO measurement was used, as this value already contains the heliocentric correction. Out of the seven obtained spectra, two radial velocities and corresponding errors were obtained for four of them. The results are displayed in Table 3. Spectrum 4 was used as a template and thus could not be used to obtain measurements. Spectrum 3 was obtained at a phase of 0.924 and thus the atomic lines were severely blended. FXCOR could not determine two distinct radial velocity measurements for this spectrum. Through the FXCOR analysis of Spectrum 7, the different wavelength ranges returned drastically different shifts. Due to the inconsistencies in the returned radial velocities, Spectrum 7 was excluded.

Spectrum Number	Radial Velocity (km/s)	Standard Deviation (km/s)
1	-157.976	11.988
	122.754	8.477
2	-114.290	23.945
	113.457	15.798
3	-	-
	-	-
4	-	-
	-	-
5	-118.871	13.512
	127.581	12.527
6	-115.685	13.207
	144.144	24.092
7	-	-
	-	-

Table 3. Radial velocities determined using FXCOR. Spectra 3 and 7 were excluded due to inconsistent measurements. Spectrum 4 was used as a template and thus could not be used to determine radial velocities.

4. BINARY ANALYSIS

The binary analysis was conducted in *PHOEBE* (PHysics of Eclipsing BinariEs) (Prša & Zwitter (2005)). The first task was to build a forward model. The values reported in the literature were inputted as initial values. Along with this, the semi-major axis of the system was set by visually inspecting the radial velocity curve. Once the initial values were tweaked to moderately match the data, optimizers were run to refine the system parameters. The parameters were optimized using the Nelder-Mead solver. The Nelder-Mead method of minimization was first proposed by Nelder & Mead (1965) however, the *PHOEBE* optimizer utilizes a wrapper on scipy.optimize, which utilizes the algorithm developed by Gao & Han (2012). Since the radial velocity curve only consists of 4 data points for each star, when running optimizers they contribute little to the overall optimization. Therefore, radial velocity parameters (including mass ratio and semi-major axis) were optimized using just the radial velocity curve. These values were then fixed and the other system parameters were optimized using the light curve and the radial velocity curve. Overall, the optimized values are inclination, mass ratio, fillout factor, temperature ratio and semi-major axis. Table 4 displays the optimized values for these parameters. Figure 3, 4 and 5 display the model outputs created using these optimized parameters including a mesh plot, a light curve and a radial velocity curve.

Parameter	Optimized Value
Inclination	72.475°
Mass Ratio	0.83154
Fillout Factor	0.042579
T_{eff} Ratio	0.96036
Semi-Major Axis	4.9534 $R_\odot$

Table 4. List of optimized parameters and their values

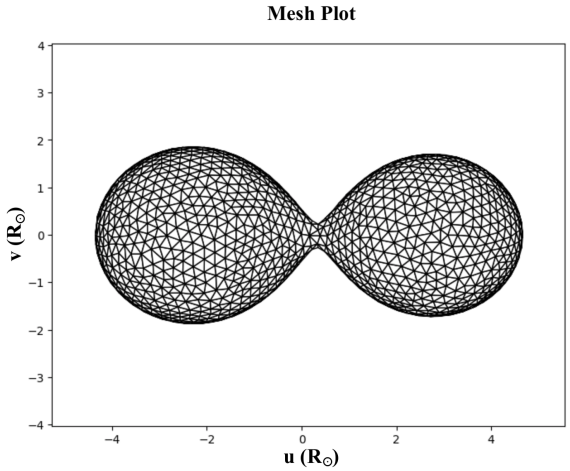

Figure 3. Graphic Representation of KIC 7766185 displayed face on at a phase of 0.25.

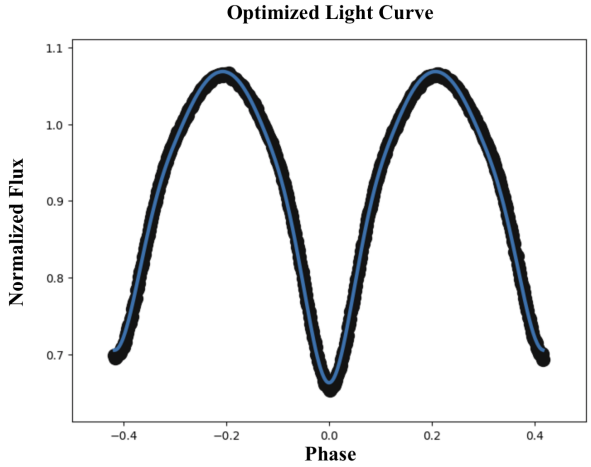

Figure 4. *Kepler* light curve with the model light curve (blue line) created using the optimized parameters

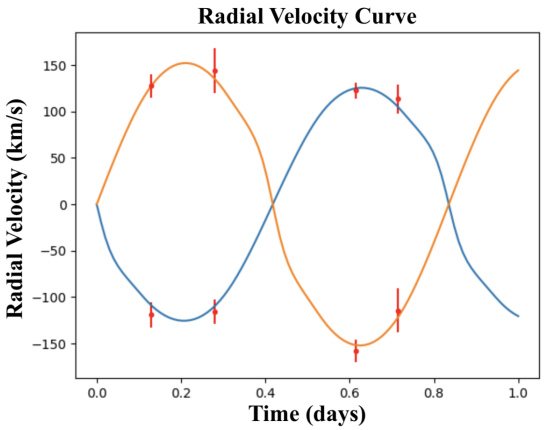

Figure 5. Radial velocity measurements (red data points) along with the model radial velocity curves created using the optimized parameters.

While the Nelder-Mead Optimizer can be used to determine error ranges on the system parameters, they are underestimated. To obtain appropriate error ranges on the optimized parameters, MCMC (Markov Chain Monte Carlo) sampling was used. A pedagogical review of MCMC sampling is given in Hogg & Foreman-Mackey (2018). MCMC is used to sample probability density functions (PDFs). In the context of *PHOEBE*, MCMC is used to fairly sample the posterior PDF ($p(\theta|D)$), or the PDF for the parameters (θ) given the data (D). A set of prior distributions may also be added to the sampler. This would be used if there is any prior knowledge on a parameter, such as a reliable estimate from the literature. This sampling gives appropriate errors on system parameters and further refines the parameter values. *PHOEBE* utilizes the MCMC sampler *emcee* developed by Foreman-Mackey et al. (2013).

Due to the small amount of radial velocity measurements, radial velocity parameters were sampled first using just the radial velocity curve. The parameters sampled were the mass ratio and $a \sin i$. The first MCMC sample was run with 16 walkers for 3000 iterations. To assess convergence, corner plots and log probability plots were analyzed. Corner plots are used to observe the posterior distributions. If convergence is reached, the distributions should be complete Gaussians. The log probability plots computes the log probability for each walker at each iteration. At each iteration, the mean log probability is plotted with a spread of one standard deviation. For convergence, after the burn-in, the log probability plot should show no upward or downward trends, only a random spread around a central value. If a log probability plot displays trends then more iterations are required. Figure 7 displays the corner plot and the log probability plot for the first MCMC run. Both plots show the requirements for convergence.

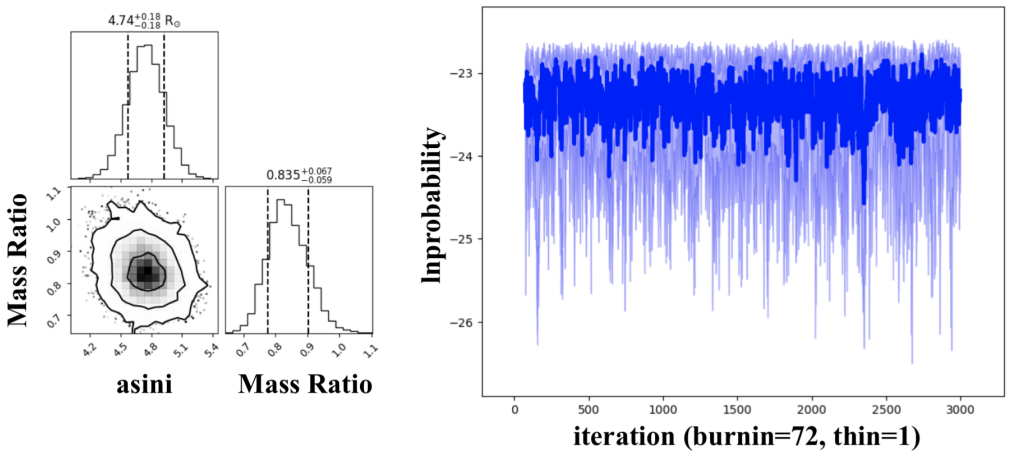

Figure 6. Corner plots (left) and log probability plot (right) for the first MCMC run, sampling only the radial velocity parameters. For the log probability plot, the dark blue line represents the mean log probability value while the light blue is a one sigma spread.

The first MCMC run returned a value for $a \sin i$ of $4.74 \pm 0.18\ R_\odot$ and a value for mass ratio of $0.835^{+0.067}_{-0.059}$. A second MCMC run was conducted to sample over the light curve parameters. The parameters sampled during the second run were fillout factor, inclination, temperature ratio and passband luminosity (pblum). During the optimizers, the pblum mode was set to dataset scaled. However, for sampling, the pblum mode was set to component coupled to accurately sample over different pblum values. The second run included prior distributions. The $a \sin i$ distribution determined from the first MCMC run was included as a prior. A prior on fillout factor was also included to prevent the walkers from traversing into the semi-detached state. For the fillout factor prior, a uniform distribution from 0.02 - 0.1 was added. Unfortunately, at this time, the second MCMC run has not converged. Figure 7 displays the corner plots and log probability plot for this run. The Gaussian distributions are clearly still taking shape and the log probability plot has a pronounced upward trend indicating that convergence has not been reached. At this time, appropriate error bars cannot be attached to light curve parameters.

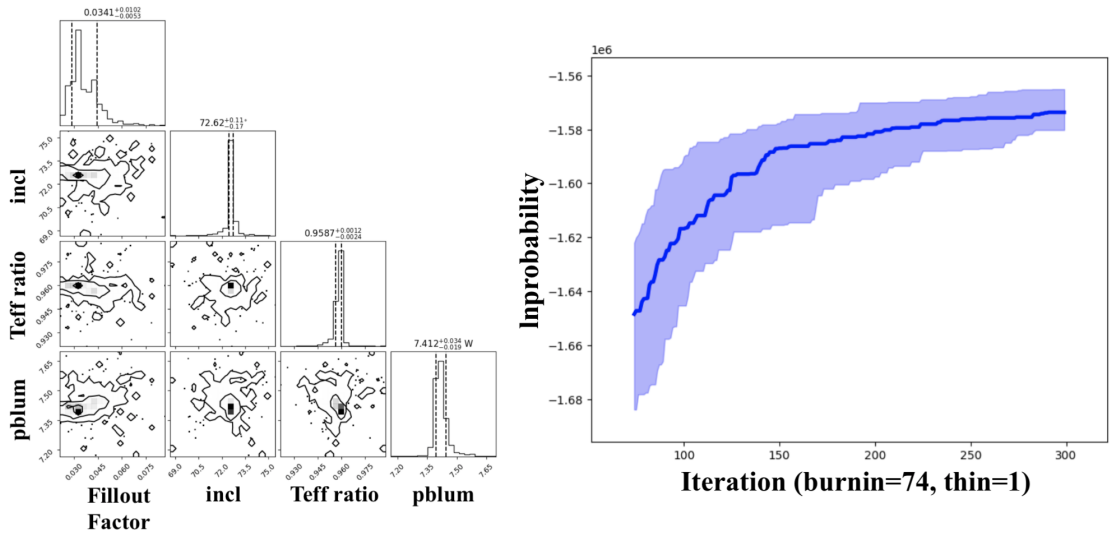

Figure 7. Corner plots (left) and log probability plot (right) for the second MCMC run. The requirements for convergence are not met and more iterations are needed. For the log probability plot, the dark blue line represents the mean log probability value while the light blue is a one sigma spread.

The system parameters for KIC 7766185 determined in this study are presented in Table 5. The radial velocity parameters have errors determined from MCMC sampling. Error ranges were omitted for light curve parameters as the second MCMC sampling did not converge yet. The values for the light curve parameters were determined from the optimizers. Note that the value for eccentricity was not determined from this study but assumed. Due to the close proximity of the stars in contact binaries, their orbits have circularized (Prša et al. (2011)).

Parameter	Value
Mass Ratio	$0.835^{+0.067}_{-0.059}$
$a \sin i$	$4.74 \pm 0.18\ R_\odot$
semi-major axis	$4.97^{+0.19}_{-0.18}\ R_\odot$
$M_{primary}$	$1.29^{+0.19}_{-0.15}\ M_\odot$
$M_{secondary}$	$1.08^{+0.13}_{-0.12}\ M_\odot$
Ω^*	$3.46^{+0.11}_{-0.1}$
Fillout Factor	0.042579
$R_{equiv,\ primary}$	$1.9864\ R_\odot$
$R_{equiv,\ secondary}$	$1.8287\ R_\odot$
inclination	72.475^o
eccentricity (assumed)	0
T_{eff} Ratio	0.96036

Table 5. System parameters of KIC 7766185 determined from this study. Error ranges are included for radial velocity parameters. Appropriate error ranges could not be applied to the light-curve parameters since the second MCMC run has not converged yet.
* Ω is the dimensionless Roche potential of the common envelope from the primary star's reference.

5. PERIOD STUDY

The structure, evolution and origin of contact binaries is an area of active research. There have been many theoretical attempts to explain these systems, including Thermal Relaxation Oscillation (TRO) and Angular Momentum Loss (AML). With multiple competing theories, period studies of contact binaries are important since the two main theories (TRO and AML) predict different mass transfer rates which are indicated by period changes (Qian (2001)). To

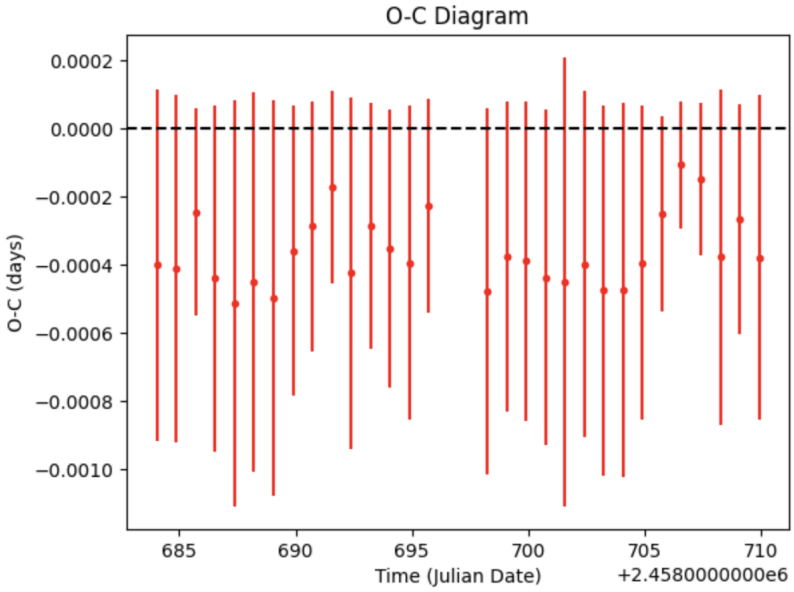

Figure 8. O-C diagram created using the *TESS* light curve

determine any period variations of KIC 7766185, an O-C diagram was constructed. Using the *TESS* Sector 14 light curve, the times of minimum for the primary eclipse were measured using the Find Extremum function in *Peranso*. O-C is the observed time of eclipse minus the calculated time of eclipse, which is calculated with the following equation:

$$O - C = T - (T_0 + nP) = T - (2454954.554702 + n * 0.8354573) \quad (2)$$

Where T is the observed time of eclipse, T_0 is the ephemeris, n is the current epoch and P is the period. The ephemeris and period value were obtained from the *Kepler Eclipsing Binary Catalog*. The O-C diagram is displayed in Figure 8.

Analyzing the O-C diagram reveals no upward or downward trends. Therefore, there is no period variations throughout the *TESS* Sector 14 observations and no period change between the *Kepler* measurements (2013) and the *TESS* measurements (2019). The data points consistently lie below the x-axis. This indicates that the ephemeris value provided by the *Kepler Eclipsing Binary Catalog* is incorrect. This value is $2454954.554702 \pm 0.041523$ Julian Date. The new proposed ephemeris which centers the O-C diagram on the x-axis is 2454954.55433995 Julian Date, which lies within the error range of the old value. Using this value for ephemeris centers the data points around an O-C value of zero (Figure 9).

6. DISCUSSION

This study conducted the first in-depth binary analysis of KIC 7766185 using both photometric and spectroscopic observations. Compared to the values reported in Prša et al. (2011), the values determined for mass ratio and temperature ratio are in good agreement, with a percent difference of 2.07% and 1.84% respectively. The values determined for inclination deviates from the reported data with a percent difference of 7.07%. The largest deviation from the literature is the fillout factor. The determined value (0.04257) has a percent difference of 126.591% from the value reported in Prša et al. (2011) (0.18943). These results demonstrate the importance of in depth studies of contact binaries to not only determine absolute parameters, but to refine the parameters reported in large pipeline studies.

From the binary analysis, the sub-type of KIC 7766185 is determined. Since we do not have multiple light curves in multiple filters, the absolute temperature of both stars cannot be determined. However, by using the *Kepler* temperature, we can confirm that KIC 7766185 is not a B-type system. If we take the primary temperature to be the *Kepler* temperature of 5977 K, then the secondary temperature is 5740 K. The temperature difference is 237 K. While the temperature reported by *Kepler* is not reliable as a primary temperature, it can be used to rule out KIC 7766185 as a B-type system. As stated in Csizmadia & Klagyivik (2004), B-type systems typically have a temperature difference of greater than 1,000 K. With a temperature ratio of 0.96036, the primary temperature would have to be

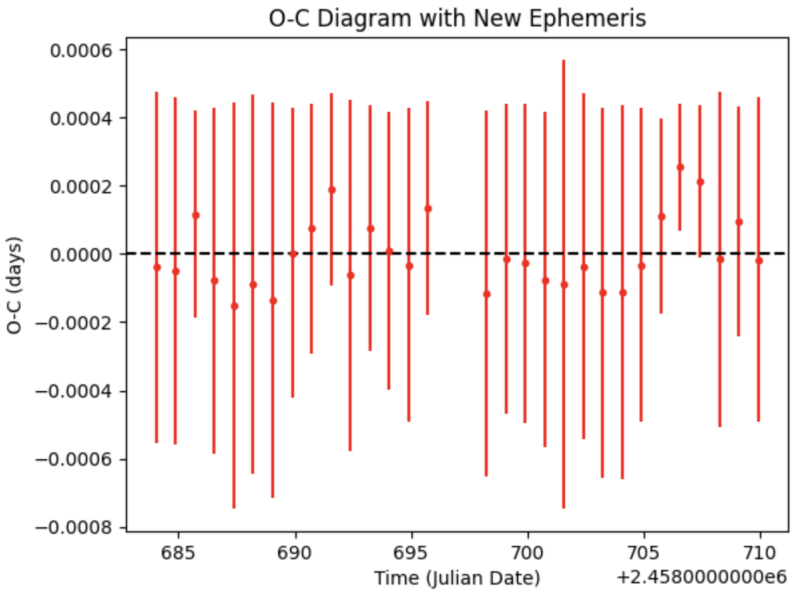

Figure 9. O-C diagram created using the corrected ephemeris of 2454954.55433995 Julian date

25,227 K (a nonphysical value for this system) before the temperature difference between the primary and secondary becomes greater than 1,000 K. Therefore, KIC 7766185 is not a B-type system and the stars are in thermal contact.

KIC 7766185 is an A-type W UMa system. A-Type systems occur when the hotter star is the larger star. The temperature ratio is defined as T_2/T_1, therefore, with a value of 0.96036, the primary (T_1) is hotter. The equivalent radius of the primary (1.9864 $R_\odot$) is larger than the equivalent radius of the secondary (1.8287 $R_\odot$). Therefore, the primary star is the hotter and larger component, verifying KIC 7766185 as an A-type W Uma star.

The period analysis did not determine any period variations for KIC 7766185. One motivation of this section was to determine if KIC 7766185 is a red nova candidate. If orbit decay continues after contact is achieved, contact binaries may undergo a full merger (Gazeas et al. (2021)). This was the case with V1309 Scorpii, which was a contact binary that underwent orbit decay until merging into a single star, igniting a red nova (Tylenda, R. et al. (2011)). Orbital period variations could indicate that the stars are still undergoing orbit decay, making KIC 7766185 a red nova candidate. However, analysis of the O-C diagram (Figure 8) reveals no period changes between the *Kepler* and *TESS* observations. Therefore, KIC 7766185 is not a red nova candidate. The data points in the O-C curve lie below the x-axis, indicating that the ephemeris reported in the *Kepler Eclipsing Binary Catalog* is incorrect. This study determines a value of 2454954.55433995 Julian Date for the new ephemeris of KIC 7766185.

7. CONCLUSION

This study conducted the first photometric and spectroscopic study of KIC 7766185. Spectra obtained from the Mayall 4-m telescope were resolved into radial velocity measurements. The radial velocity curve and the *Kepler* light curve were used in *PHOEBE* to perform binary analysis. This study determined the first set of absolute stellar parameters for KIC 7766185. These parameters confirm the system as an A-type W UMa star. The period analysis determined no period variations between the *Kepler* and *TESS* observations. As of now, KIC 7766185 is not a red nova candidate since no period decay was discovered. Future observations are needed to determine the absolute temperatures of KIC 7766185. Photometry in multiple filters will allow the determination of primary and secondary effective temperatures, which can be appended to the list of absolute parameters determined by this study.

8. ACKNOWLEDGEMENTS

The author would like to thank Dr. Scott Engle, Dr. Angela Kochoska and Dr. Andrej Prša from the Villanova Department of Astronomy and Planetary Science for continuous support and guidance throughout this project.

REFERENCES

Alpaslan, M. 2009, arXiv e-prints, arXiv:0912.4755

Binnendijk, L. 1965, Veroeffentlichungen der Remeis-Sternwarte zu Bamberg, 27, 36

Borucki, W. J., Koch, D., Basri, G., & et al. 2010, Science, 327, 977, doi: 10.1126/science.1185402

Brown, A. G. A., Vallenari, A., Prusti, T., et al. 2021, Astronomy & Astrophysics, 650, doi: 10.1051/0004-6361/202039657e

Brown, T. M., Latham, D. W., Everett, M. E., & Esquerdo, G. A. 2011, AJ, 142, 112, doi: 10.1088/0004-6256/142/4/112

Csizmadia, S., & Klagyivik, P. 2004, Astronomy & Astrophysics, 426, 1001–1005, doi: 10.1051/0004-6361:20040430

Eker, Z., Demircan, O., & Bilir, S. 2008, Monthly Notices of the Royal Astronomical Society, 386, 1756–1758, doi: 10.1111/j.1365-2966.2008.13155.x

Foreman-Mackey, D., Hogg, D. W., Lang, D., & Goodman, J. 2013, Publications of the Astronomical Society of the Pacific, 125, 306, doi: 10.1086/670067

Frasca, A., Molenda-Zakowicz, J., De Cat, P., et al. 2016, A&A, 594, A39, doi: 10.1051/0004-6361/201628337

Gao, F., & Han, L. 2012, Computational Optimization and Applications, 51, 259, doi: 10.1007/s10589-010-9329-3

Gazeas, K., & Stępień, K. 2008, Monthly Notices of the Royal Astronomical Society, 390, 1577, doi: 10.1111/j.1365-2966.2008.13844.x

Gazeas, K. D., Loukaidou, G. A., Niarchos, P. G., et al. 2021, Monthly Notices of the Royal Astronomical Society, 502, 2879–2892, doi: 10.1093/mnras/stab234

Høg, E., Fabricius, C., Makarov, V. V., et al. 2000, A&A, 355, L27

Hogg, D. W., & Foreman-Mackey, D. 2018, The Astrophysical Journal Supplement Series, 236, 11, doi: 10.3847/1538-4365/aab76e

KPNO. 2021, Mayall Telecope Parameters, http://www-kpno.kpno.noao.edu/kpno-misc/mayall_params.html

Lucy, L. B. 1968, Astrophysical Journal, 151, 1123, doi: 10.1086/149510

Nelder, J. A., & Mead, R. 1965, The Computer Journal, 7, 308, doi: 10.1093/comjnl/7.4.308

Paunzen, E., & Vanmunster, T. 2016, Astronomische Nachrichten, 337, 239, doi: 10.1002/asna.201512254

Prša, A., Batalha, N., Slawson, R. W., et al. 2011, The Astronomical Journal, 141, 83, doi: 10.1088/0004-6256/141/3/83

Prša, A., & Zwitter, T. 2005, Astrophysical Journal, 628, 426, doi: 10.1086/430591

Qian, S. 2001, Monthly Notices of the Royal Astronomical Society, 328, 914, doi: 10.1046/j.1365-8711.2001.04921.x

Ricker, G. R., Winn, J. N., Vanderspek, R., et al. 2015, Journal of Astronomical Telescopes, Instruments, and Systems, 1, 014003, doi: 10.1117/1.JATIS.1.1.014003

Ruciński, S. 1986, Symposium - International Astronomical Union, 118, 159–172, doi: 10.1017/S0074180900151307

Terrell, D., Gross, J., & Jr, W. 2012, The Astronomical Journal, 143, 99, doi: 10.1088/0004-6256/143/4/99

Tody, D. 1986, in Instrumentation in Astronomy VI, ed. D. L. Crawford, Vol. 0627, International Society for Optics and Photonics (SPIE), 733 – 748. https://doi.org/10.1117/12.968154

Tonry, J., & Davis, M. 1979, AJ, 84, 1511, doi: 10.1086/112569

Tylenda, R., Hajduk, M., Kamiński, T., et al. 2011, Astronomy & Astrophysics, 528, A114, doi: 10.1051/0004-6361/201016221